AIAA JOURNAL
Vol. 33, No. 3, March 1995

Vibration and Buckling of Flexible Rotating Beams

Chris D. Eick*
AlliedSignal Engines, Phoenix, Arizona 85072–2181
and
Marc P. Mignolet†
Arizona State University, Tempe, Arizona 85287-6106

Perturbation techniques are employed to estimate the free vibration characteristics and buckling limit of a flexible rotating Bernoulli–Euler beam. The normalized beam stiffness $\varepsilon = EI/m\Omega^2\bar{R}^4$ is introduced and treated as a small parameter. Then, singular perturbation solutions to the governing eigenvalue problem are derived that are valid up to and including order ε for any given hub radius. The special case of a zero hub radius is then considered and the corresponding solutions are presented. Next, a transformation is introduced which leads to a regular perturbation formulation of the problem the solution of which is presented. The natural frequency/mode shape predictions and buckling limits obtained from both the singular and regular perturbation formulations are compared with "exact" values obtained from a power series solution of the eigenvalue problem. The singular perturbation solution matches well with the "exact" values for small stiffnesses whereas the regular perturbation solution provides an excellent accuracy for all beam stiffnesses and hub radii considered.

I. Introduction

THE determination of the dynamic response of rotating beams, i.e., mode shapes, natural frequencies, etc., is an important prerequisite in the design of helicopter and turbomachinery blades (see Ref. 1 for an extensive literature review). In this context, it has often been observed that the parameter $\varepsilon = EI/m\Omega^2\bar{R}^4$, which quantifies the relative magnitude of the restoring force provided by the beam stiffness (EI) with respect to the centripetal effect ($m\Omega^2\bar{R}^4$), is small, e.g., of the order of 0.004 for helicopter blade applications.[2] This situation has quite naturally led to the formulation of perturbation-based approximations of the natural frequencies and mode shapes of the beam but also of its buckling limit.

Among the first published results in this area that rely on singular perturbation techniques are those of Colin[3] and Peters[4] who studied outward-facing cantilever beams, for which the support is the closest point of the beam to the center of rotation (see Fig. 1), with zero hub radius, i.e., $\bar{a} = 0$. In the former investigation,[3] approximations of the first two natural frequencies and mode shapes are presented that are valid to order $\varepsilon^{\frac{1}{2}}$ for $\varepsilon \ll 1$. The latter study,[4] yielded order $\varepsilon^{\frac{1}{2}}$ natural frequency and mode shape expansions for all modes and an order ε approximation for the first mode. In addition, a large stiffness expansion was developed in Ref. 4 which can be combined with the previously derived small stiffness limit to obtain a global approximation of the natural frequencies. The mathematical aspects of the eigenvalue problem have been studied in detail by Lakin[5] and Lakin and Ng[6] who rigorously developed natural frequency expansions up to order $\varepsilon^{\frac{1}{2}}$ along with mode shape approximations. These results verified and extended the expansions given in Ref. 3 and 4. The case of a nonzero hub radius, $\bar{a} \neq 0$, was investigated by Hodges[7] who developed a general approximation of the first natural frequency by combining the $\bar{a} \approx 0$ and $\bar{a} \approx \bar{R}$ limiting cases.

The related problem of the vibration and buckling of an inward-facing rotating beam, for which some or all of the points of the beam are closer to the center of rotation than is the support (see Fig. 1), has also been investigated by perturbation techniques. In particular, an asymptotic approximation of the transverse buckling limit was developed by Nachman[8] whereas the limiting behavior, as $\varepsilon \to 0$, of the natural frequencies of vibration was investigated by Lakin.[9] A general approach was then devised by these authors[10,11] to analyze both vibration and buckling of an inward facing beam in a single framework. This new procedure relies on the dual role of the eigenvalues, i.e., either the vibration natural frequencies or the growth rates for buckling. An interesting conclusion from these studies is that buckling is possible even when the beam is fully under tension, i.e., $\bar{R} > |\bar{a}|$ and $\bar{a} < 0$. An order $\varepsilon^{\frac{1}{2}}$ composite expansion of the buckling limit valid for all values of stiffness and hub radii was developed by Peters and Hodges[12] who confirmed that buckling is possible for beams fully under tension. Additional related work, on the buckling and vibration of a rotating spoke having clamped boundary conditions at both ends, has been completed by Lakin et al.[13] and Lakin and Nachman.[14]

The purpose of this investigation is to present a unified and thorough treatment of the vibration characteristics and buckling limit of inward/outward-facing rotating beams. Specifically, perturbation-like approximations of the natural frequencies, mode shapes, and the buckling limit will be derived by extending and generalizing the method used in Ref. 4. Also, and more importantly, a new solution strategy that involves a regular perturbation problem will be presented. It is hoped that the physical aspects of the vibration and buckling of rotating beams brought up by the present perturbation techniques will ultimately be used to improve the computational techniques for the dynamic analysis of helicopter and turbomachinery blades.

II. Rotating Beam Differential Equation

In this section, the differential equation governing the small amplitude motions of a rotating Bernoulli–Euler beam is developed. Both transverse and in-plane cases are discussed for beams facing inward or outward as shown in Fig. 1. Although vibration and buckling are separate problems, they can be analyzed in a unique framework by associating the buckling limit with a vanishing natural frequency of vibration.

The differential equation governing small amplitude motions of the constant cross section beams shown in Fig. 1 is

$$EI\frac{\partial^4 w}{\partial \bar{x}^4} - \frac{1}{2}m\Omega^2\frac{\partial}{\partial \bar{x}}\left[(\bar{R}^2 - \bar{x}^2)\frac{\partial w}{\partial \bar{x}}\right] = \begin{cases} -m\dfrac{\partial^2 w}{\partial t^2}, & \text{transverse} \\ -m\dfrac{\partial^2 w}{\partial t^2} + m\Omega^2 w, & \text{in plane} \end{cases} \tag{1}$$

where m denotes the beam's mass per unit length and EI its flexural

Received Sept. 28, 1993; revision received Jan. 24, 1994; accepted for publication April 20, 1994.

*Senior Engineer, Component Design.
†Associate Professor, Department of Mechanical and Aerospace Engineering.

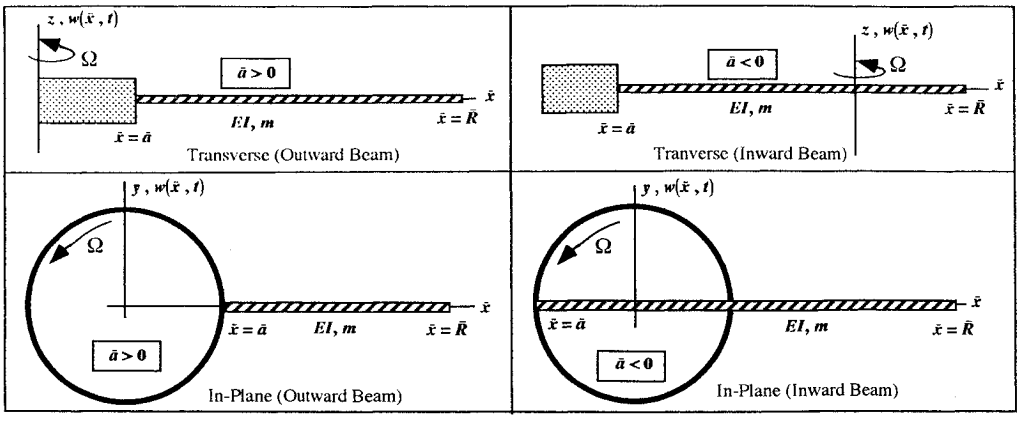

Fig. 1 In-plane/transverse rotating beam configurations.

rigidity. Further, $w(\bar{x}, t)$ is the time varying displacement component at a location $\bar{x}$, and Ω is the beam's angular velocity. The boundary conditions associated with Eq. (1) correspond to the existing supports. In the present investigation, it is assumed that the beam is clamped at $\bar{x} = \bar{a}$ and free at $\bar{x} = \bar{R}$ so that

$$w(\bar{a}, t) = 0, \qquad \frac{\partial w}{\partial \bar{x}}(\bar{a}, t) = 0, \qquad \frac{\partial^2 w}{\partial \bar{x}^2}(\bar{R}, t) = 0 \qquad \frac{\partial^3 w}{\partial \bar{x}^3}(\bar{R}, t) = 0 \tag{2}$$

Introducing the dimensionless quantities $x = \bar{x}/\bar{R}$ and $\tau = \Omega t$, and assuming a harmonic solution of the form $w(x, \tau) = X(x) \exp(i\omega\tau)$, it is found that Eqs. (1) and (2) reduce to

$$\varepsilon \frac{d^4X}{dx^4} - \frac{1}{2}\frac{d}{dx}\left[(1 - x^2)\frac{dX}{dx}\right] - \lambda X = 0 \tag{3}$$

and

$$X(a) = 0, \qquad \frac{dX}{dx}(a) = 0, \qquad \frac{d^2X}{dx^2}(1) = 0 \qquad \frac{d^3X}{dx^3}(1) = 0 \tag{4}$$

where $\varepsilon = EI/m\Omega^2\bar{R}^4$ is the beam's normalized stiffness, $a = \bar{a}/\bar{R}$, and

$$\lambda = \begin{cases} \omega^2, & \text{transverse vibrations} \\ \omega^2 + 1, & \text{in-plane vibrations} \end{cases} \tag{5}$$

In addition, a normalization condition

$$X(1) = 1 \tag{6}$$

is imposed on the mode shape.

In a vibration analysis, ε is a known quantity and Eqs. (3) and (4) constitute a standard eigenvalue problem which possesses a nontrivial solution only for specific values of λ. Each such λ yields a corresponding natural frequency ω and a mode shape $X(x)$. When studying buckling, it is noted that the term $\exp(i\omega\tau)$ grows unbounded with increasing time τ whenever $\omega^2 < 0$. Thus, the stability limit is the value of ε which results in zero natural frequencies, i.e., $\omega = 0$.

III. Solution Methods

In this section three techniques for solving the eigenvalue problem will be presented: an "exact" approach based on power series and both singular and regular perturbation methods.

A. "Exact" Solution

An "exact" numerical solution to Eq. (3) can be developed by relying on a power series expansion similar to the ones used by Stafford and Giurgiutiu,[15] Giurgiutiu and Stafford,[16] and Wright et al.[17] Specifically, the solution $X(x)$ is sought in the form of a power series about the ordinary point $x = 1$, i.e.,

$$X(x) = \sum_{n=0}^{\infty} \alpha_n (1 - x)^n \tag{7}$$

Applying the boundary conditions (4) and the normalization condition (6) to the preceding solution yields a nonlinear algebraic equation in the two parameters ε and λ.

The numerical aspects of the solution of this equation for either the eigenvalue λ or the critical stiffness ε_{cr} deserve some attention. Specifically, the appearance of the stiffness ε in the denominator of the recurrence relation for α_n (Ref. 25) has been found to lead to an ill conditioning when $\varepsilon \ll 1$. The critical value of the stiffness below which numerical difficulties are encountered depends on the algorithm selected, but it is typically of order $\varepsilon \approx 0.001$. These computational difficulties are not unexpected since in the limit $\varepsilon \to 0$ the order of the governing differential equation reduces from four to two with a change in boundary conditions, from Eq. (4) to zero and bounded displacements at the clamped and free ends, respectively. A similar situation, i.e., decreased accuracy as $\varepsilon \to 0$, has also been encountered when Eq. (3) is solved by using energy methods and is discussed in Ref. 4.

For vibration analysis, ε is known beforehand, and the nonlinear equation is solved for the eigenvalue λ. The mode shape is then determined from Eq. (7). Finally, the corresponding natural frequency is computed from Eq. (5).

The power series method can also be used to determine the buckling limit. However, in this case, the value of the parameter λ is known, it corresponds to $\omega = 0$ through Eq. (5), whereas the beam's normalized stiffness is to be determined. This computation is achieved by solving for ε, the critical stiffness, as the sole unknown.

B. Singular Perturbation Solution

In many practical situations, the beam's normalized stiffness ε is small with respect to unity. Thus, it is quite natural to seek solutions of Eq. (3) by relying on the limiting case $\varepsilon = 0$. In this context, however, note that the degree of the differential equation (3) drops from 4 to 2 as ε vanishes. Following standard arguments,[18] it can be shown that the solution of Eq. (3) with $\varepsilon = 0$ closely approximates its $\varepsilon \neq 0 (0 < \varepsilon \ll 1)$ counterpart in the so-called outer domain consisting of the entire interval $x \in (a, 1)$ from which small neighborhoods of the two boundaries, the inner domains or boundary layers, are excluded. Further, the behavior of the solution in these small boundary layers is dictated by the parameter ε. This fundamental role is best revealed by performing a coordinate stretching. Proceeding in this manner yields three different differential equations which are each valid in one part of the domain $[a, 1]$.

A matching procedure can then be used to patch the three separate solutions into a single composite approximation.[18]

This procedure has been followed by Peters[4] in the case $a = 0$ to obtain an order ε approximation of the first natural frequency of the beam and order $\varepsilon^{\frac{1}{2}}$ approximations of the remaining ones (the "combined" expressions given in Ref. 4). The derivation of higher order approximations and the case $a \neq 0$ was not presented, probably because of the serious mathematical difficulties it entails. In the present investigation, some new results[19] will be used to demonstrate how an approximation of any order in ε can be obtained for both cases $a = 0$ and $a \neq 0$. Further, some discrepancies between Refs. 4 and 6 will be presented and resolved.

Governing Equations

Following the preceding discussion, introduce first the change of variables $\xi = (x - a)/\varepsilon^{\gamma}$ into Eq. (3). Then, balancing dominant terms for ε small and ξ finite, it is found that $\gamma = \frac{1}{2}$ and that the inner equation around $x = a$ is

$$\frac{d^4X^i}{d\xi^4} - \frac{1}{2}\frac{d}{d\xi}\left[\left(1 - a^2 - 2a\varepsilon^{\frac{1}{2}}\xi - \varepsilon\xi^2\right)\frac{dX^i}{d\xi}\right] - \varepsilon\lambda X^i = 0 \quad (8)$$

with the boundary conditions

$$X^i(\xi = 0) = 0, \qquad \frac{dX^i(\xi = 0)}{d\xi} = 0 \quad (9)$$

corresponding to the first two relations of Eq. (4). Proceeding similarly near the tip, a transformation $\eta = (1 - x)/\varepsilon^{\nu}$ leads to $\nu = \frac{1}{3}$, and the corresponding inner equation around $x = 1$ is

$$\frac{d^4X^I}{d\eta^4} - \frac{1}{2}\frac{d}{d\eta}\left[\left(2\eta - \varepsilon^{\frac{1}{3}}\eta^2\right)\frac{dX^I}{d\eta}\right] - \varepsilon^{\frac{1}{3}}\lambda X^I = 0 \quad (10)$$

with boundary conditions dictated by the last two relations in Eq. (4) and the normalization requirement, Eq. (6), i.e.,

$$\frac{d^2X^I(\eta = 0)}{d\eta^2} = 0, \qquad \frac{d^3X^I(\eta = 0)}{d\eta^3} = 0, \qquad X^I(\eta = 0) = 1 \quad (11)$$

Finally, no transformation is required in the outer region, so that

$$\varepsilon\frac{d^4X^o(x)}{dx^4} - \frac{1}{2}\frac{d}{dx}\left[(1 - x^2)\frac{dX^o(x)}{dx}\right] - \lambda X^o(x) = 0 \quad (12)$$

for $x \in (a, 1)$. Note that there is no boundary condition associated with the outer equation since the corresponding domain of definition does not include $x = a$ or $x = 1$.

The next step in the process is to assume that the solutions in the inner and outer regions can be expressed as power series of the parameter ε. The terms $\varepsilon^{\frac{1}{3}}$, $\varepsilon^{\frac{1}{2}}$, and ε in Eqs. (8), (10), and (12) suggest expanding the functions $X^o(x)$, $X^i(\xi)$, $X^I(\eta)$ and the parameter λ in powers of $\varepsilon^{\frac{1}{6}}$, or equivalently,

$$X^o(x) = \sum_{s=0}^{\infty}\varepsilon^{s/6}X_s^o(x) \quad (13)$$

$$X^i(\xi) = \sum_{s=0}^{\infty}\varepsilon^{s/6}X_s^i(\xi) \quad (14)$$

$$X^I(\eta) = \sum_{s=0}^{\infty}\varepsilon^{s/6}X_s^I(\eta) \quad (15)$$

$$\lambda = \sum_{s=0}^{\infty}\varepsilon^{s/6}\lambda_s \quad (16)$$

Introducing Eqs. (13–16) into Eqs. (8–12) produces three differential equations which must be solved at each power of $\varepsilon^{\frac{1}{6}}$. Each equation will be discussed separately in the following sections.

Inner Domain at $x = a$

Introducing the expansions (14) and (16) into Eqs. (8) and (9) yields the recursive set of differential equations

$$\frac{d^4X_s^i}{d\xi^4} - \alpha^2\frac{d^2X_s^i}{d\xi^2} = -a\frac{d}{d\xi}\left[\xi\frac{dX_{s-3}^i}{d\xi}\right] - \frac{1}{2}\frac{d}{d\xi}\left[\xi^2\frac{dX_{s-6}^i}{d\xi}\right] + \sum_{n=0}^{s-6}\lambda_n X_{s-n-6}^i, \qquad s = 0, 1, 2, \ldots \quad (17)$$

and the boundary conditions

$$X_s^i(\xi = 0) = 0, \qquad \frac{dX_s^i}{d\xi}(\xi = 0) = 0 \quad (18)$$

where $X_s^i \equiv 0$ for $s < 0$, and $\alpha = \sqrt{(1 - a^2)/2}$. It should be noted from Eq. (17) that all solutions $X_s^i(\xi)$ share the same homogenous part

$$\left[X_s^i(\xi)\right]_h = \tilde{a}_s + \tilde{b}_s\xi + \tilde{c}_s e^{-\alpha\xi} + \tilde{d}_s e^{\alpha\xi} \quad (19)$$

where $\tilde{a}_s$, $\tilde{b}_s$, $\tilde{c}_s$, and $\tilde{d}_s$ are unknown constants to be determined by the boundary conditions and the matching process. Further, the particular solution can be found by the method of undetermined coefficients and consists of polynomials in ξ and products of polynomials in ξ by $e^{-\alpha\xi}$ and similar terms with $e^{\alpha\xi}$.

Outer Region

Inserting the perturbation expansions Eqs. (13) and (16) into Eq. (12) and comparing powers of ε yield the recursive set of differential equations

$$(1 - x^2)\frac{d^2X_s^o}{dx^2} - 2x\frac{dX_s^o}{dx} + \nu(\nu + 1)X_s^o = -2\sum_{j=1}^{s}\lambda_j X_{s-j}^o + 2\frac{d^4X_{s-6}^o}{dx^4}, \qquad s = 0, 1, 2, \ldots \quad (20)$$

where the substitution $\lambda_0 = \nu(\nu + 1)/2$ has been made and $X_s^o \equiv 0$ for $s < 0$. As stated previously, the outer equation is not required to satisfy any boundary condition. Note again, that the differential operator appearing on the left-hand-side of Eq. (20) is the same for all values of s. Thus, the homogenous parts of $X_s^o(x)$ are all the same and can be expressed in terms of the Legendre functions $P_\nu(x)$ and $Q_\nu(x)$ as

$$\left[X_s^o(x)\right]_h = a_s P_\nu(x) + b_s Q_\nu(x) \quad (21)$$

where a_s and b_s are arbitrary constants to be determined in the matching process. Note that the function $Q_\nu(x)$ can be expressed as the sum of two terms which are regular and singular, respectively, at $x = 1$. Further, the singular part can be written as $P_\nu(x)\ln(1 - x)$.

In view of Eq. (21), the solution of Eq. (20) at any order s can be written as

$$X_s^o(x) = a_s P_\nu(x) + b_s Q_\nu(x) + \left[X_s^o(x)\right]_p \quad (22)$$

where $[X_s^o(x)]_p$ is the particular solution of Eq. (20) at order s. It can be found by the method of reduction of order since the homogenous solution is known. Specifically, introducing an assumed solution of the form $[X_s^o(x)]_p = P_\nu(x)h(x)$ into Eq. (20) and integrating twice yields

$$\left[X_s^o(x)\right]_p = P_\nu(x)\int_1^x\left\{\frac{1}{[P_\nu(u)]^2(1 - u^2)}\int_1^u f_s(t)P_\nu(t)\,dt\right\}du \quad (23)$$

where $f_s(x)$ denotes the right-hand side of Eq. (20) at order s. The choice of the integration limits in Eq. (23), from 1 to u, eliminates any singularities of the integrand at $u = 1$. Further, any singularity at the zeros of $P_\nu(u)$ is eliminated through the multiplication by $P_\nu(x)$. Therefore, the particular solution $[X_s^o(x)]_p$ is well defined and finite for all values of x and s. It was found that the particular solution corresponding to $s = 3$, i.e., $[X_3^o(x)]_p$, could be expressed as $\lambda_3[\partial P_\nu/\partial\lambda]_{\lambda=\lambda_0}$ (Ref. 25).

Inner Domain at $x = 1$

Introducing the expansions (15) and (16) into Eqs. (10) and (11) yields the recursive set of differential equations

$$\frac{d^4X_s^I}{d\eta^4} - \frac{d}{d\eta}\left[\eta\frac{dX_s^I}{d\eta}\right] = -\frac{1}{2}\frac{d}{d\eta}\left[\eta^2\frac{dX_{s-2}^I}{d\eta}\right] + \sum_{j=0}^{s-2}\lambda_j X_{s-2-j}^I, \qquad s = 0, 1, 2, \ldots \tag{24}$$

with boundary and normalization conditions

$$\frac{d^2X_s^I}{d\eta^2}(\eta = 0) = 0, \qquad \frac{d^3X_s^I}{d\eta^3}(\eta = 0) = 0$$

$$X_s^I(\eta = 0) = \begin{cases} 1, & s = 0 \\ 0, & s > 0 \end{cases} \tag{25}$$

where $X_s^I \equiv 0$ for $s < 0$. As already seen in connection with the two previous solutions, the homogenous part of $X_s^I(\eta)$ is the same for each order s and can be expressed as

$$[X_s^I(\eta)]_h = \hat{b}_s\int_0^\eta Ai(t)\,dt + \hat{c}_s\int_0^\eta Bi(t)\,dt + \hat{d}_s - \pi\hat{a}_s\int_0^\eta Gi(t)\,dt \tag{26}$$

where $Ai(t)$, $Bi(t)$, and $Gi(t)$ denote Airy functions.[20] The constants $\hat{a}_s$, $\hat{b}_s$, $\hat{c}_s$, and $\hat{d}_s$ are arbitrary and will be determined by the boundary conditions and the matching process. The particular solutions corresponding to any order s can easily be found, using the method described in Ref. 19, as linear combinations of products of polynomials in η and derivatives of the homogenous part $[X_s^I(\eta)]_h$.

Matching

It should be noted that enforcing all of the boundary and normalization conditions does not lead to a unique solution for the functions $X_s^o(x)$, $X_s^i(\xi)$, and $X_s^I(\eta)$. This conclusion results from the existence, at any order s, of only five boundary and normalization conditions for 10 arbitrary constants, a_s, b_s, $\hat{a}_s$, $\hat{b}_s$, $\hat{c}_s$, $\hat{d}_s$, $\tilde{a}_s$, $\tilde{b}_s$, $\tilde{c}_s$, and $\tilde{d}_s$. In fact, these parameters should also be selected so that the transition from an inner solution to the outer one is as smooth as possible. This matching procedure requires that the inner expansions for large values of the inner variable be equal to the outer expansion for values of the outer variable corresponding to the boundary layer.[18] For $s = 0$, this requirement can be expressed as

$$\lim_{\xi\to\infty} X_0^i(\xi) = \lim_{x\to a} X_0^o(x) \tag{27}$$

$$\lim_{\eta\to\infty} X_0^I(\eta) = \lim_{x\to 1} X_0^o(x) \tag{28}$$

It should be noted that the right-hand side of Eqs. (17), (20), and (24) vanish for $s = 0$. Thus, the solutions $X_0^i(\xi)$, $X_0^o(x)$, and $X_0^I(\eta)$ are given by Eqs. (19), (21), and (26). Further, applying the boundary and normalization conditions, Eqs. (18) and (25), it is found that the matching conditions, Eqs. (27) and (28), can be expressed as

$$\lim_{\xi\to\infty}\left\{-(\tilde{c}_0 + \tilde{d}_0) + \alpha(\tilde{c}_0 - \tilde{d}_0)\xi + \tilde{c}_0 e^{-\alpha\xi} + \tilde{d}_0 e^{\alpha\xi}\right\} = \lim_{x\to a}\{a_0 P_\nu(x) + b_0 Q_\nu(x)\} \tag{29}$$

and

$$\lim_{\eta\to\infty}\left\{\hat{c}_0\int_0^\eta Bi(t)\,dt + \sqrt{3}\,\hat{c}_0\int_0^\eta Ai(t)\,dt + 1\right\} = \lim_{x\to 1}\{a_0 P_\nu(x) + b_0 Q_\nu(x)\} \tag{30}$$

Examining Eq. (29) first, it is seen that the term $e^{\alpha\xi}$ grows exponentially and cannot be matched to the outer solution since both $P_\nu(x)$ and $Q_\nu(x)$ are finite at $x = a$. Thus, the coefficient $\tilde{d}_0$ must be set to zero. A similar argument can be made about the integral of $Bi(t)$ in Eq. (30) so that $\hat{c}_0 = 0$. Finally, the term $Q_\nu(x)$ in Eq. (30) grows logarithmically near $x = 1$ requiring that $b_0 = 0$. Noting that $P_\nu(1) = 1$ for all ν (Ref. 21), Eqs. (29) and (30) are satisfied only when $\tilde{c}_0 = 0$, $a_0 = 1$, and $P_\nu(a) = 0$. The various solutions for $s = 0$ are then

$$X_0^o(x) = P_\nu(x), \qquad X_0^i(\xi) = 0, \qquad X_0^I(\eta) = 1, \qquad \lambda_0 = \nu(\nu+1)/2 \tag{31}$$

where ν is determined from the equation $P_\nu(a) = 0$.

The matching proceeds in a similar fashion up to order $\varepsilon^{\frac{5}{6}}$. At order ε, however, it can be shown that for all cases such that $\lambda_0 \neq 1$, the coefficient $\hat{a}_6$ does not vanish, and the term

$$-\hat{a}_6\pi\int_0^\eta Gi(t)\,dt \tag{32}$$

remains in the inner solution $X_6^I(\eta)$. During the matching process it is necessary to avail the asymptotic expansion of Eq. (32) for large η. In fact, it can be shown[22] that

$$\int_0^\eta Gi(t)\,dt \approx \frac{2\gamma + \ell n(3)}{3\pi} + \frac{1}{\pi}\ell n(\eta) \qquad \text{for large } \eta \tag{33}$$

where γ is Euler's constant. Rewriting the preceding expression in terms of the outer variable x yields

$$\int_0^{\frac{1-x}{\varepsilon^{1/3}}} Gi(t)\,dt \approx \frac{2\gamma + \ell n 3}{3\pi} + \frac{1}{\pi}\left[\ell n(1-x) - \frac{1}{3}\ell n\varepsilon\right] \tag{34}$$

for x near 1 and $\varepsilon \ll 1$. To match the term $\ell n(1-x)$, it is necessary to retain the term $b_6 Q_\nu(x)$ which also displays a $\ell n(1-x)$ behavior near $x = 1$. It remains to accommodate the term $(\ell n\,\varepsilon)/3$. To this end, note that there is no such term in any of the assumed perturbation expansions (13–16). Thus, it is necessary to modify these equations by including an $\varepsilon\,\ell n\,\varepsilon$ term in the perturbation series. That is, let

$$X^o(x) = \sum_s \varepsilon^{s/6}X_s^o(x) + \varepsilon\,\ell n\,\varepsilon X_*^o(x) \tag{35}$$

$$X^i(\xi) = \sum_s \varepsilon^{s/6}X_s^i(\xi) + \varepsilon\,\ell n\,\varepsilon X_*^i(\xi) \tag{36}$$

$$X^I(\eta) = \sum_s \varepsilon^{s/6}X_s^I(\eta) + \varepsilon\,\ell n\,\varepsilon X_*^I(\eta) \tag{37}$$

$$\lambda = \sum_s \varepsilon^{s/6}\lambda_s + \varepsilon\,\ell n\,\varepsilon\lambda_* \tag{38}$$

Using these new representations, it is possible to achieve a satisfactory matching at order ε. The analytic expressions of the solutions $X_s^o(x)$, $X_s^i(\xi)$, $X_s^I(\eta)$, and λ_s corresponding to an arbitrary clamping radius a, are presented in Table 1.

Special Case $a = 0$

Significant simplifications occur when $a = 0$. In particular, the zeroth-order frequency equation becomes $P_\nu(0) = 0$ which is satisfied only when ν is an odd positive integer, i.e., $\nu = 1, 3, 5, \ldots$ (Ref. 20). Then, the corresponding Legendre functions reduce to the corresponding Legendre polynomials, the first two of which are $P_1(x) = x$ and $P_3(x) = (5x^3 - 3x)/2$. Further, the inner and outer solutions can be determined in closed form using special functions, i.e., the Airy and the DiLogarithm[23] functions. Specifically, these solutions, and the corresponding eigenvalues, were obtained for the first two mode shapes and are presented in Tables 2 and 3, respectively.

Examining the expressions presented in Tables 2 and 3, note that there is no $\varepsilon\,\ell n\,\varepsilon$ contribution to the functions $X^o(x)$, $X^i(\xi)$, $X^I(\eta)$, and the parameter λ for the first mode whereas there exists a nonzero term $X_*^o(x)$ for the second one. This situation is a direct consequence

Table 1 Singular perturbation mode shapes and eigenvalues for arbitrary a

s	Order	$X_s^i(\xi)$	$X_s^o(x)$	$X_s^I(\eta)$	λ_s
0	ε^0	0	$P_\nu(x)$	1	$\frac{\nu(\nu+1)}{2}: P_\nu(a)=0$
1	$\varepsilon^{\frac{1}{6}}$	0	0	0	0
2	$\varepsilon^{\frac{1}{3}}$	0	0	$-\lambda_0\eta$	0
3	$\varepsilon^{\frac{1}{2}}$	$\tilde{a}_3\{1-\alpha\xi-\exp(-\alpha\xi)\}$	$\lambda_3\left[\frac{\partial P_\nu}{\partial\lambda}\right]_{\lambda=\lambda_0}$	0	$-\frac{1}{\alpha}\frac{\left[\frac{\partial P_\nu}{\partial x}\right]_{x=a}}{\left[\frac{\partial P_\nu}{\partial\lambda}\right]_{\lambda=\lambda_0}}$
4	$\varepsilon^{\frac{2}{3}}$	0	$-\left(\frac{\lambda_0^2-\lambda_0}{6Ai'(0)}\right)P_\nu(x)$	$\left(\frac{\lambda_0^2-\lambda_0}{4}\right)\eta^2+\hat{X}_{41}(\eta)$	0
5	$\varepsilon^{\frac{5}{6}}$	0	0	$-\lambda_3\eta$	0
6	ε	$\tilde{a}_6[1-\alpha\xi-\exp(-\alpha\xi)]$ $-\frac{a\tilde{a}_3}{4\alpha}\xi^2[2+\exp(-\alpha\xi)]$ $+\frac{3a\tilde{a}_3}{4\alpha^2}\xi[1-\exp(-\alpha\xi)]$	$a_6P_\nu(x)$ $-\hat{a}_6Q_\nu(x)$ $+X_{6p}(x)$	$\hat{b}_6\int_0^\eta Ai(t)\,dt$ $-\pi\hat{a}_6\int_0^\eta Gi(t)\,dt$ $+\hat{d}_6+\hat{X}_{6p}(\eta)$	Obtain from solving: $\lim_{x\to a}X_{6p}(x)=\tilde{a}_6$ $+\hat{a}_6Q_\nu(a)$
*	$\varepsilon\ln\varepsilon$	0	$(\hat{a}_6/3)\,P_\nu(x)$	0	0

$$X_{41}(\eta)=-\frac{\left(\lambda_0^2-\lambda_0\right)}{2Ai'(0)}\int_0^\eta Ai(t)\,dt$$

$$\tilde{a}_6=\frac{1}{\alpha}\left\{\frac{3}{4}a\frac{\tilde{a}_3}{\alpha^2}-\lambda_3\left[\frac{\partial^2P_\nu}{\partial x\partial\lambda}\right]_{x=a}\right\}$$

$$\alpha=\sqrt{\frac{(1-a^2)}{2}}$$

$$\hat{b}_6=\frac{1}{Ai'(0)}\left[\hat{a}_6\pi Gi'(0)-\frac{\left(\lambda_0^2-\lambda_0\right)\left(\lambda_0-\frac{1}{10}\right)Ai(0)}{2Ai'(0)}\right]$$

$$\hat{a}_6=-\frac{\left(\lambda_0^2-\lambda_0\right)(2\lambda_0+3)}{6}$$

$$\tilde{a}_3=-\frac{1}{\alpha}\left[\frac{\partial P_\nu(x)}{\partial x}\right]_{x=a}$$

$$\hat{X}_{6p}(\eta)=-\lambda_0\eta X_{41}(\eta)-\frac{1}{10}\eta^2\frac{dX_{41}(\eta)}{d\eta}+\left(\lambda_0+\frac{3}{10}\right)\frac{d^2X_{41}(\eta)}{d\eta^2}-\left(\frac{\lambda_0^2-\lambda_0}{4}\right)\left(\frac{\lambda_0-3}{9}\right)\eta^3$$

$$\hat{d}_6=\left(\lambda_0+\frac{3}{10}\right)\times\left(\frac{\lambda_0^2-\lambda_0}{2}\right)$$

$$X_{6p}(x)=-2P_\nu(x)\int_1^x\left\{\frac{1}{(1-t^2)[P_\nu(t)]^2}\int_1^t[\lambda_3X_3(s)+\lambda_6P_\nu(s)-P_\nu''''(s)]P_\nu(s)\,ds\right\}dt$$

$$a_6=\frac{\hat{b}_6}{3}-\hat{a}_6\left(\frac{2\gamma+\ln 3}{3}\right)+\hat{d}_6$$

of the unit value of the parameter λ_0. Indeed, when $\lambda_0=1$, significant simplifications result from the vanishment of the $(\lambda_0^2-\lambda_0)$ term which occurs frequently in Table 1. These observations can be used to resolve an apparent discrepancy between the work by Peters[4] and the papers by Lakin[5] and Lakin and Ng.[6] Specifically, the former study did not include any $\varepsilon\ln\varepsilon$ term in the expansions of $X^o(x)$, $X^i(\xi)$, $X^I(\eta)$, and λ whereas the latter investigations did. In this respect, note that Peters' study included an order ε correction only for the first mode for which no nonzero $\varepsilon\ln\varepsilon$ term is present as seen from Table 2. On the other hand, Lakin[5] and Lakin and Ng[6] have hypothesized the inclusion of $\varepsilon\ln\varepsilon$ contributions but have not carried out their analysis far enough to determine these terms or to notice that they vanish for the first mode. The present work clarifies these past efforts by explicitly demonstrating that $\varepsilon\ln\varepsilon$ terms are present for all cases except when $\lambda_0=1$, which occurs only for the first mode and when $a=0$.

Vibration

In a vibration study, it is necessary to estimate the natural frequencies and mode shapes. The former quantities are determined from Eq. (5) with the approximation

$$\lambda=\lambda_0+\varepsilon^{\frac{1}{2}}\lambda_3+\varepsilon\lambda_6 \tag{39}$$

Finally, the mode shapes are determined from the composite expansions of $X^o(x)$, $X^i(\xi)$, and $X^I(\eta)$.

Buckling

The singular perturbation buckling solution proceeds in an identical manner as the vibration solution. Specifically, the beam will buckle if the natural frequency of the first mode shape computed from Eqs. (5) and (39) is purely imaginary. Further, to determine the critical value of ε below which a beam would buckle, it is sufficient to compute the lowest solution, $\varepsilon=\varepsilon_{cr}$ of the quadratic equation

$$\lambda_0+\varepsilon_{cr}^{\frac{1}{2}}\lambda_3+\varepsilon_{cr}\lambda_6=\begin{cases}0, & \text{transverse}\\ 1, & \text{in plane}\end{cases} \tag{40}$$

C. Regular Perturbation Solution

To motivate the forthcoming regular perturbation approach to the solution of Eq. (3), consider first the limiting case $a\to 1$. In the singular perturbation section, it was found that the boundary layer thickness is proportional to $\varepsilon^{\frac{1}{2}}$ at $x=a$ and $\varepsilon^{\frac{1}{3}}$ at $x=1$. Since $\varepsilon\ll 1$, it follows that $\varepsilon^{\frac{1}{3}}>\varepsilon^{\frac{1}{2}}$ and the free edge boundary layer is thicker than its clamping radius counterpart. On this basis, it can be expected that as $a\to 1$, the boundary layer at $x=1$ will be the first to cover the entire domain $[a,1]$. Thus, whenever the normalized beam length, $1-a$, is of the order of $\varepsilon^{\frac{1}{3}}$, the response of the beam should be governed only by the inner equation at $x=1$. Under this assumption, the governing differential equation becomes

$$\frac{d^4X(\eta)}{d\eta^4}-\frac{1}{2}\frac{d}{d\eta}\left[\left(2\eta-\varepsilon^{\frac{1}{3}}\eta^2\right)\frac{dX(\eta)}{d\eta}\right]-\varepsilon^{\frac{1}{3}}\lambda X(\eta)=0 \tag{41}$$

with the boundary and normalization conditions

$$X(\Delta)=0,\qquad X'(\Delta)=0,\qquad X''(0)=0$$
$$X'''(0)=0,\qquad X(0)=1 \tag{42}$$

Table 2 Singular perturbation mode 1 shape and eigenvalues for $a = 0$

s	Order	$X_s^i(\xi)$	$X_s^o(x)$	$X_s^I(\eta)$	λ_s
0	ε^0	0	x	1	1
1	$\varepsilon^{\frac{1}{6}}$	0	0	0	0
2	$\varepsilon^{\frac{1}{3}}$	0	0	$-\eta$	0
3	$\varepsilon^{\frac{1}{2}}$	$\sqrt{2}\left\{\frac{\xi}{\sqrt{2}} - 1 + \exp\left[-\frac{\xi}{\sqrt{2}}\right]\right\}$	$\sqrt{2}\left\{x - 1 + x\,\ell n\left(\frac{1+x}{2}\right)\right\}$	0	$\frac{3\sqrt{2}}{2}$
4	$\varepsilon^{\frac{2}{3}}$	0	0	0	0
5	$\varepsilon^{\frac{5}{6}}$	0	0	$-(3\sqrt{2}/2)\eta$	0
6	ε^1	$2(1-\ell n\,2)\times\left\{\frac{\xi}{\sqrt{2}} - 1 + \exp\left[-\frac{\xi}{\sqrt{2}}\right]\right\}$	$\frac{2\lambda_6}{3}\left[x - 1 + x\,\ell n\left(\frac{1+x}{2}\right)\right] + \frac{8}{3}\left\{1 - x + \left[\frac{3}{4} + \frac{x}{2}\right]\ell n\left(\frac{1+x}{2}\right)\right\} - 2x\,\text{polylog}\left\{2, \frac{1-x}{2}\right\}$	0	$7 - 6\,\ell n\,2$
*	$\varepsilon\,\ell n\,\varepsilon$	0	0	0	0

where $\Delta = (1-a)/\varepsilon^{\frac{1}{3}}$. Since the small parameter ε only appears in Eq. (41) through $\varepsilon^{\frac{1}{3}}$, a perturbation expansion of the function $X(\eta)$ of the form

$$X(\eta) = \sum_{s=0}^{\infty} \varepsilon^{s/3} X_s(\eta) \tag{43}$$

is justified. To determine the correct form of the series representation of the eigenvalues λ, an asymptotic, $a \to 1$, analysis of the singular perturbation results presented in Table 1 was performed.[25] This analysis suggested the expansion

$$\lambda = \sum_{s=-1}^{\infty} \varepsilon^{s/3} \lambda_s \tag{44}$$

The presence of a negative power of ε could have been expected since in the limit $a \to 1$, or equivalently $\varepsilon \to 0$ for a fixed Δ, the beam is characterized by infinite natural frequencies.

The essence of the present regular perturbation technique is to rely on the expansions (43) and (44) for all values of a, not only $a \approx 1$. This procedure is indeed a regular perturbation technique since it is readily shown that Eq. (41) does not support any boundary layer for finite values of Δ.

Combining Eqs. (41), (43), and (44) yields the following set of differential equations:

$$\frac{d^4 X_s(\eta)}{d\eta^4} - \frac{d}{d\eta}\left[\eta \frac{dX_s(\eta)}{d\eta}\right] - \lambda_{-1} X_s(\eta) = -\frac{1}{2}\frac{d}{d\eta}\left[\eta^2 \frac{dX_{s-1}(\eta)}{d\eta}\right] + \sum_{j=0}^{s-1} \lambda_j X_{s-1-j}(\eta), \qquad s = 0, 1, \ldots \tag{45}$$

where $X_s \equiv 0$ for $s < 0$. For $s = 0$, Eq. (45) reduces to

$$\frac{d^4 X_0(\eta)}{d\eta^4} - \frac{d}{d\eta}\left[\eta \frac{dX_0(\eta)}{d\eta}\right] - \lambda_{-1} X_0(\eta) = 0 \tag{46}$$

the solution of which can be sought in the form of a power series about the ordinary point $\eta = 0$, i.e.,

$$X_0(\eta) = \sum_{j=0}^{\infty} \gamma_j \eta^j \tag{47}$$

Introducing this assumed solution in Eq. (46), it is found that the coefficients γ_j must satisfy the recurrence relation

$$\gamma_{j+4} = \frac{(j+1)^2 \gamma_{j+1} + \lambda_{-1}\gamma_j}{(j+4)(j+3)(j+2)(j+1)}, \qquad j = 0, 1, \ldots \tag{48}$$

Four linearly independent solutions to Eq. (46), denoted by $V_0(\eta)$, $V_1(\eta)$, $V_2(\eta)$, and $V_3(\eta)$, can be obtained by setting $\gamma_0 = 1$, $\gamma_1 = \gamma_2 = \gamma_3 = 0$ for $V_0(\eta)$; $\gamma_1 = 1$, $\gamma_0 = \gamma_2 = \gamma_3 = 0$ for $V_1(\eta)$; etc. The general solution to Eq. (46) is then

$$X_0(\eta) = \delta_{00} V_0(\eta) + \delta_{10} V_1(\eta) + \delta_{20} V_2(\eta) + \delta_{30} V_3(\eta) \tag{49}$$

where δ_{00}, δ_{10}, δ_{20}, and δ_{30} are unknown constants. Applying the boundary and normalization conditions (42) yields the values $\delta_{00} = 1$, $\delta_{20} = \delta_{30} = 0$, and the two relations

$$\begin{aligned} V_0(\Delta) + \delta_{10} V_1(\Delta) &= 0 \\ V_0'(\Delta) + \delta_{10} V_1'(\Delta) &= 0 \end{aligned} \tag{50}$$

The preceding system of linear algebraic equations possesses a solution only when

$$V_0(\Delta) V_1'(\Delta) - V_0'(\Delta) V_1(\Delta) = 0 \tag{51}$$

For a given value of Δ, the preceding condition represents in fact a nonlinear algebraic equation for the eigenvalue λ_{-1}. Once this parameter has been computed by solving Eq. (51), the constant δ_{10} is determined from Eq. (50) yielding the mode shape $X_0(\eta)$ in the form

$$X_0(\eta) = V_0(\eta) + \delta_{10} V_1(\eta) \tag{52}$$

The determination of the corrections $X_1(\eta)$ and λ_0, $X_2(\eta)$ and $\lambda_1, \ldots$, proceeds in a manner analogous to the singular perturbation case. Specifically, note that the left-hand side of Eq. (45) is the same for all values of s. Thus, the homogenous parts, $[X_s(\eta)]_h$, can all be expressed in the form of Eq. (49). Further, the method described in Ref. 19 can be used to produce particular solutions that consist of products of polynomials in η and of derivatives of the function $X_0(\eta)$, Eq. (52). In particular, for $s = 1$ it is found that

$$[X_1(\eta)]_p = -\frac{(5 + 30\lambda_0 + 8\eta\lambda_{-1})}{30\lambda_{-1}} X_0'''(\eta) + \frac{2}{15} X_0''(\eta) + \frac{(32\lambda_{-1}^2 + 5\eta + 30\lambda_0\eta + 5\lambda_{-1}\eta^2)}{30\lambda_{-1}} X_0'(\eta) + \frac{\eta}{6} X_0(\eta) \tag{53}$$

Table 3 Singular perturbation mode 2 shape and eigenvalues for $a = 0$

s	Order	$X_s^i(\xi)$	$X_s^o(x)$	$X_s^I(\eta)$	λ_s
0	ε^0	0	$P_3(x)$	1	6
1	$\varepsilon^{\frac{1}{6}}$	0	0	0	0
2	$\varepsilon^{\frac{1}{3}}$	0	0	-6η	0
3	$\varepsilon^{\frac{1}{2}}$	$-\frac{3\sqrt{2}}{2}\left\{\frac{\xi}{\sqrt{2}} - 1 + \exp\left[-\frac{\xi}{\sqrt{2}}\right]\right\}$	$\lambda_3 X_p(x)$	0	$\frac{63\sqrt{2}}{8}$
4	$\varepsilon^{\frac{2}{3}}$	0	$5(3)^{\frac{1}{3}}\Gamma\left(\frac{1}{3}\right)P_3(x)$	$X_4^I(\eta)$	0
5	$\varepsilon^{\frac{5}{6}}$	0	0	$-(63\sqrt{2}/8)\eta$	0
6	ε	$\left(\frac{-45+54\,\ell n\,2}{8}\right) \times \left\{\frac{\xi}{\sqrt{2}} - 1 + \exp\left[-\frac{\xi}{\sqrt{2}}\right]\right\}$	$a_6 P_3(x) + 75 Q_3(x) + \lambda_6 X_p(x) + X_{6p}(x)$	$\hat{X}_6(\eta)$	$\frac{4713 - 567\,\ell n\,2}{8}$
*	$\varepsilon\,\ell n\,\varepsilon$	0	$-25P_3(x)$	0	0

$$X_p(x) = \frac{4}{21} - \frac{5x}{14} - \frac{5x^2}{7} + \frac{37x^3}{42} + \frac{2}{7}P_3(x)\,\ell n\left(\frac{1+x}{2}\right)$$

$$X_4^I(\eta) = \frac{15\eta^2}{2} + 15(3)^{\frac{1}{3}}\Gamma\left(\tfrac{1}{3}\right)\int_0^\eta Ai(t)\,dt$$

$$Q_3(x) = -\frac{4}{3} + \frac{11x}{2} + 5x^2 - \frac{55x^3}{6} + P_3(x)\left[\ell n(1-x) - \ell n\left(\frac{1+x}{2}\right)\right]$$

$$a_6 = \frac{189}{2} + 50\gamma + \frac{25\sqrt{3}}{3}\pi - \frac{59\left[\Gamma\left(\frac{1}{3}\right)\right]^2}{2\Gamma\left(\frac{2}{3}\right)} + 25\,\ell n\,3$$

$$\hat{X}_6(\eta) = \hat{b}_6\int_0^\eta Ai(t)\,dt + 75\pi\int_0^\eta Gi(t)\,dt + \frac{189}{2} - \frac{5}{2}\eta^3 + \frac{189}{2Ai'(0)}Ai'(\eta) + \frac{3}{2Ai'(0)}\eta^2 Ai'(\eta) + \frac{90}{Ai'(0)}\eta\int_0^\eta Ai(t)\,dt$$

$$\hat{b}_6 = -\frac{59}{\left[\Gamma\left(\frac{1}{3}\right)\right]^2} + \frac{150\pi\Gamma\left(\frac{1}{3}\right)}{2\sqrt{3}\Gamma\left(\frac{2}{3}\right)}$$

$$X_{6p}(x) = -\frac{369}{56} + \frac{4401}{448}x + \frac{5157}{224}x^2 - \frac{11763}{448}x^3 - \left[\frac{27}{4} + \frac{2349}{224}x - \frac{405}{16}x^2 - \frac{6183}{224}x^3\right]\ell n\left(\frac{1+x}{2}\right) + \frac{81}{16}P_3(x)\,\text{polylog}\left\{2, \frac{1-x}{2}\right\}$$

A two-term approximate solution of the eigenvalue problem, Eqs. (41) and (42), is then obtained as

$$X(\eta) = X_0(\eta) + \varepsilon^{\frac{1}{3}}X_1(\eta) \tag{54}$$

and

$$\lambda = \frac{\lambda_{-1}}{\varepsilon^{\frac{1}{3}}} + \lambda_0 \tag{55}$$

where

$$X_1(\eta) = \delta_{01}V_0(\eta) + \delta_{11}V_1(\eta) + \delta_{21}V_2(\eta) + \delta_{31}V_3(\eta) + \left[X_1(\eta)\right]_p \tag{56}$$

The five unknowns appearing in Eq. (56), i.e., λ_0, δ_{01}, δ_{11}, δ_{21}, and δ_{31}, are determined by applying the five boundary/normalization conditions (42) and solving the resulting linear system of algebraic equations.

In a vibration study, it is necessary to determine the natural frequencies and mode shapes of the rotating beam. The stiffness ε is then known and the parameter Δ can be computed as $\Delta = (1-a)/\varepsilon^{\frac{1}{3}}$. Then, following the previous discussion, the mode shapes and eigenvalues are given by Eqs. (54) and (55). Finally, the corresponding natural frequencies are determined from Eq. (5).

This procedure can also be used to test if the beam will buckle. This phenomenon will occur if the natural frequency corresponding to the first mode is purely imaginary. Finally, note that an approximation of the buckling limit is readily available by selecting λ according to Eq. (5). Then, Eq. (55) yields the critical value of ε as

$$\varepsilon_{cr} = \left(\frac{\lambda_{-1}}{\lambda - \lambda_0}\right)^3 \tag{57}$$

The asymptotic behavior of the parameter $\lambda_{-1} = \lambda_{-1}(\Delta)$ as $\Delta \to 0$ and $\Delta \to \infty$ can be determined as follows. In the case $\Delta \to 0$, corresponding to either $a \to 1$ or $\varepsilon \to \infty$, it is expected that the centripetal effects will be negligible with respect to the bending ones. This assumption leads to the classical frequency equation for a cantilever beam as

$$\cos\left[\sqrt[4]{\frac{\lambda}{\varepsilon}}(1-a)\right]\cosh\left[\sqrt[4]{\frac{\lambda}{\varepsilon}}(1-a)\right] + 1 = 0 \tag{58}$$

the roots of which are

$$\sqrt[4]{\frac{\lambda}{\varepsilon}}(1-a) = \beta_n \tag{59}$$

where β_n are the well-known nonrotating clamped-free beam frequencies.

Solving Eq. (59) for λ and comparing to Eq. (55) yields the desired asymptotic relationship as

$$\lambda_{-1} \to \frac{\beta_n^4}{\Delta^4}, \qquad \text{as } \Delta \to 0 \tag{60}$$

Considering the first mode, it is found that $\beta_1 = 1.8751$ and thus $\beta_1^4 = 12.36$.

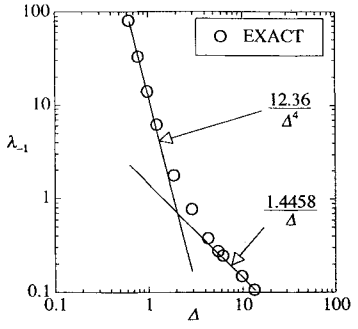

Fig. 2 Comparision between exact and predicted asymptotic relationships for λ_{-1}.

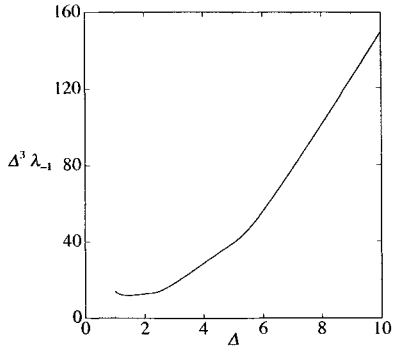

Fig. 3 Exact values of λ_{-1} between asymptotic domains.

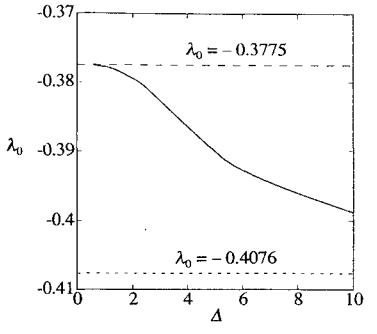

Fig. 4 Exact value of λ_0 for mode 1.

The case $\Delta \to \infty$ corresponds to $\varepsilon \to 0$. Thus, comparing Eqs. (31), (39), and (55) it is expected that

$$\frac{\lambda_{-1}}{\varepsilon^{\frac{1}{3}}} + \lambda_0 \to \frac{\nu(\nu+1)}{2}, \qquad \text{as } \varepsilon \to 0 \tag{61}$$

where $P_\nu(a) = 0$. Note that the above asymptotic behavior holds for all values of a. Further, it can be shown that[25]

$$\frac{\nu(\nu+1)}{2} \to \frac{\mu_n^2}{4(1-a)} = \frac{\mu_n^2}{4\Delta\varepsilon^{\frac{1}{3}}}, \qquad \text{as } a \to 1 \tag{62}$$

where μ_n is the nth zero of the Bessel function J_0. Combining Eqs. (61) and (62) yields the desired asymptotic relationship

$$\lambda_{-1} \to \frac{\mu_n^2}{4\Delta}, \qquad \text{as } \Delta \to \infty \tag{63}$$

Considering the first mode, it is found[20] that $\mu_1 = 2.40483$ so that $\mu_1^2/4 = 1.4458$.

A numerical comparison of the exact values of λ_{-1} computed by Eq. (51) and the asymptotic behavior predicted by Eqs. (60) and (63), which is presented in Fig. 2 for the first mode, confirms the validity of the given limiting arguments. To permit an easy evaluation of the eigenvalue λ_{-1} given a value of Δ, the function $\lambda_{-1}(\Delta)$ is presented with linear axes in Fig. 3 for $\Delta \in [1, 10]$. Outside this domain, the asymptotic relations (60) and (63) can be used to estimate accurately λ_{-1} as seen from Fig. 2.

The determination of the limits of λ_0 as $\Delta \to 0$ or ∞ can be accomplished similarly by relying on more precise forms of the asymptotic relations (59) and (62). Consider first the limit $\Delta \to 0$. Then, Eq. (59) can be recognized from Eq. (3), as the first term of the regular perturbation representation of the eigenvalue λ for $1/\varepsilon \ll 1$. The corresponding two-term approximation can be shown to be

$$\frac{\lambda}{\varepsilon} = \frac{\beta_n^4}{1-a} + \frac{1}{\varepsilon}\left[\frac{\bar{\gamma}_n}{1-a} + \delta_n\right] \tag{64}$$

where

$$\bar{\gamma}_n = 2 - \alpha_n\beta_n + \frac{\alpha_n^2\beta_n^2}{2} \tag{65}$$

$$\delta_n = -\frac{3}{4} + \frac{\alpha_n\beta_n}{2}\left(1 - \frac{\alpha_n\beta_n}{3}\right) \tag{66}$$

and

$$\alpha_n = \frac{\cos(\beta_n) + \cosh(\beta_n)}{\sin(\beta_n) + \sinh(\beta_n)} \tag{67}$$

Proceeding as in Eqs. (59) and (60) leads to the asymptotic relation[25]

$$\frac{\lambda_{-1}}{\varepsilon^{\frac{1}{3}}} + \lambda_0 \to \frac{\beta_n^4}{1-a}\varepsilon + \frac{\bar{\gamma}_n}{1-a} + \delta_n = \left[\frac{\beta_n^4}{\Delta^4} + \frac{\bar{\gamma}_n}{\Delta}\right]\frac{1}{\varepsilon^{\frac{1}{3}}} + \delta_n \tag{68}$$

from which the following limits are easily derived:

$$\lim_{\Delta\to 0} \lambda_{-1} = \frac{\beta_n^4}{\Delta^4} + \frac{\bar{\gamma}_n}{\Delta} \tag{69}$$

$$\lim_{\Delta\to 0} \lambda_0 = \delta_n \tag{70}$$

Note that Eq. (69) represents an improved approximation of Eq. (60).

The determination of the limit of λ_0 as $\Delta \to \infty$ is accomplished as in Eq. (62) by investigation of the behavior of the expression $\nu(\nu+1)/2$ as $a \to 1$. Specifically, it can be shown that[25]

$$\frac{\nu(\nu+1)}{2} \to \frac{\mu_n^2}{4(1-a)} - \frac{1}{6}\left[1 + \frac{\mu_n^2}{4}\right] = \frac{\mu_n^2}{4\Delta\varepsilon^{\frac{1}{3}}} - \frac{1}{6}\left[1 + \frac{\mu_n^2}{4}\right] \tag{71}$$

from which it is found that

$$\lim_{\Delta\to\infty} \lambda_0 = -\frac{1}{6}\left[1 + \frac{\mu_n^2}{4}\right] \tag{72}$$

A plot of the function $\lambda_0(\Delta)$, presented in Fig. 4, clearly demonstrates the validity of the asymptotic relations (70) and (72).

IV. Numerical Results

A. Vibration

Each of the three solution methods presented in the previous section was used to solve Eqs. (3) and (4) for values of ε ranging from 0.001 to 4.0 with $a = 0.0$, 0.5, and 0.9 . In view of Eq. (5) and to ensure a maximum of generality, the forthcoming discussion will emphasize eigenvalues rather than natural frequencies. In this manner, the results presented will be applicable to both transverse and in-plane motions of the beam.

The "exact" results given in this section correspond to the power series solution with 200 terms in the expansion of $X(x)$. To assess the adequacy of this number, the eigenvalues and mode shapes were also determined by using 100 and 300 terms. In all cases presented, it was found that the eigenvalues obtained with 200 and 300 terms were identical to the first four decimal places.

The eigenvalues corresponding to $a = 0$ are given in Tables 4 and 5 for modes 1 and 2, respectively. As expected, the singular

Table 4 Mode 1 eigenvalues for $a = 0$

ε	Exact	Singular perturbation	Regular perturbation
0.001	1.07	1.07	1.10
0.004	1.15	1.15	1.17
0.010	1.25	1.24	1.27
0.040	1.66	1.54	1.67
0.100	2.42	1.95	2.42
0.400	6.14	3.48	6.14
1.000	13.55	5.96	13.55
4.000	50.64	16.61	50.64

Table 5 Mode 2 eigenvalues for $a = 0$

ε	Exact	Singular perturbation	Regular perturbation
0.001	6.78	6.89	6.90
0.004	8.36	8.86	8.44
0.010	11.3	12.5	11.4
0.040	25.9	29.8	25.9
0.100	55.0	63.5	55.0
0.400	200.7	229.1	200.7
1.000	492.0	557.2	492.0
4.000	1948.6	2188.6	1948.6

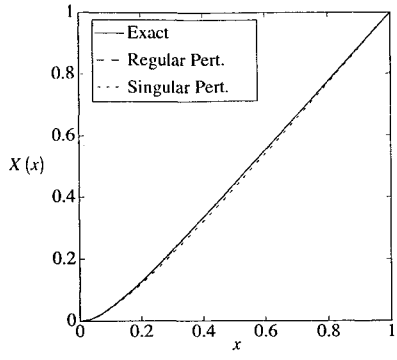

Fig. 5 Mode 1 shape for $a = 0$ and $\varepsilon = 0.004$.

perturbation method provides accurate approximations of the eigenvalues for $\varepsilon \ll 1$. Note, however, that the accuracy rapidly decreases as ε, or more surprisingly as the mode number, increases. This latter behavior is discussed in details in the Appendix where it is demonstrated that the reduction in accuracy of the singular perturbation approximation is associated with an increase, with increasing mode number, of the relative magnitude of the bending terms with respect to the centripetal ones in the outer domain. In fact, a simple analysis has shown that this relative magnitude behaves approximately as εn^2 where n denotes the mode number.

Considering next the regular perturbation method, it is found that this approach also yields very accurate estimates, but throughout the entire range of values of ε. This result is somewhat surprising since the regular perturbation method was devised initially only for $a \approx 1$ whereas the results shown in Table 4 and 5 correspond to $a = 0$.

The various approximations of the first two mode shapes corresponding to $a = 0$ and $\varepsilon = 0.004$ are presented in Figs. 5 and 6, respectively. Clearly, the singular perturbation solution yields a mode shape that is very accurate for mode 1 and slightly in error for mode 2, whereas the corresponding regular perturbation approximations are nearly identical to their exact counterparts.

The lowest eigenvalues obtained for $a = 0.5$ by relying on the exact, singular, and regular perturbation techniques are given in Table 6. Note the degradation, with respect to the case $a = 0$, of the reliability of the estimates obtained by using the singular perturbation method. The regular perturbation method, on the other hand, is as accurate as in the case $a = 0$ for all values of ε. A comparison of the mode shapes, which is not presented here for brevity, confirms all

Table 6 Mode 1 eigenvalues for $a = 0.5$

ε	Exact	Singular perturbation	Regular perturbation
0.001	2.86	2.79	2.86
0.004	3.51	3.14	3.51
0.010	4.72	3.60	4.72
0.040	10.67	5.08	10.67
0.100	22.54	7.24	22.54
0.400	81.88	15.56	81.88

Table 7 Mode 1 eigenvalues for $a = 0.9$

ε	Exact	Singular perturbation	Regular perturbation
0.001	139	38	139
0.004	510	79	510
0.010	1252	149	1252
0.040	4960	460	4960
0.100	12378	1042	12378
0.400	49465	3830	49465

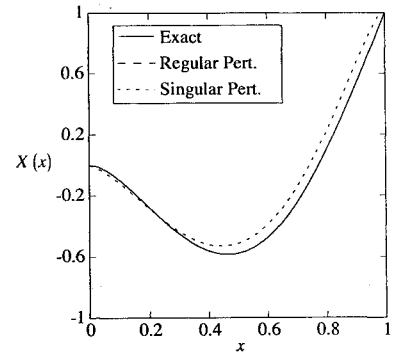

Fig. 6 Mode 2 shape for $a = 0$ and $\varepsilon = 0.004$.

of the previous observations; the accuracy of the matching between the exact curves and their singular perturbation approximation decreases as the mode number or the clamping radius a increases, whereas the regular perturbation technique yields mode shapes that are almost indistinguishable from their exact counterparts.

As a final check of the validity of these conclusions, the eigenvalues corresponding to $a = 0.9$ were computed and are presented in Table 7. A comparison of these results with those shown in Tables 4 and 6 clearly demonstrates that the accuracy of the singular perturbation estimates of the eigenvalues decreases as the clamping radius a increases whereas the regular perturbation method provides reliable approximations of these quantities for all clamping radii. Further, the same conclusion was also found to hold in connection with the mode shapes.

A simple justification of this decrease in accuracy of the singular perturbation method as $a \to 1$ can be found by considering the asymptotic behavior of the terms λ_0 and λ_3. Specifically, it is found that $\lambda_0 \propto 1/(1-a)$ and $\lambda_3 \propto 1/(1-a)^{\frac{5}{2}}$. Further, it can also be shown that λ_6 is proportional to $1/(1-a)^4$ as $a \to 1$. Thus, for a close enough to 1, an increase in the clamping radius yields an increase in the term λ_6 which is larger than its counterpart for λ_3 which, in turn, is larger than the change in the term λ_0. Thus, as a increases from 0 to 1, the high-order terms of the expansion of the eigenvalue λ become less negligible and the accuracy of the three-term approximation, Eq. (39), decreases.

B. Buckling

The buckling limit for in-plane motions was determined by all three solution methods and by the approximation techniques devised by Peters and Hodges.[12] These results are plotted in Fig. 7 using the coordinates α_w, and β_w which allow direct comparison with the work of White et al.[24] It is seen that the singular perturba-

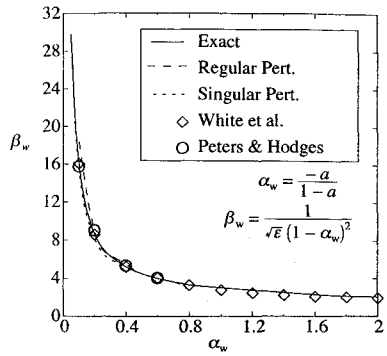

Fig. 7 In-plane buckling stability limit.

tion method predicts accurately the buckling limit for $\alpha_w < 0.5$ but does not provide any such estimate for $\alpha_w > 0.5$, or equivalently, $a < -1$. Indeed, in this case there is no real number ν satisfying the ε^0 frequency equation,[9] $P_\nu(a) = 0$, and the singular perturbation solution technique cannot be completed. Both the regular perturbation and exact solutions, on the other hand, provide an excellent agreement with the previously published results throughout the entire range of values of ε.

The determination of the in-plane buckling limit for small α_w has led to some disagreement in the literature. In Ref. 10 it was found, through numerical studies, that buckling is not possible for $\alpha_w < 0.05$ whereas Refs. 12 and 24 concluded that buckling occurs even for $\alpha_w = 0$. In fact, the asymptotic relationship giving the critical value of stiffness below which buckling occurs was developed in Ref. 12 as $\varepsilon = \alpha_w^2/2$. In applying the results of the present study, it should first be noted that for small α_w the critical stiffness ε is also small. Thus, the singular perturbation method is ideally suited to resolve the controversy. Numerically, buckling was observed for all values of $\alpha_w > 0$, thereby supporting the conclusions of Refs. 12 and 24. To confirm the asymptotic behavior $\varepsilon = \alpha_w^2/2$, a three-term Taylor approximation of the Legendre function $P_\nu(x)$ was first derived for $x \approx 0$. This expansion was then expanded with respect to ν for $\nu \approx 1$ up to and including the quadratic terms $(\nu - 1)^2$. The resulting approximation of the Legendre function $P_\nu(x)$ was relied upon to evaluate the quantities λ_0, λ_3, and λ_6 according to Table 1 for a small dimensionless hub radius a. The buckling limit was then predicted according to Eq. (40). This procedure led to the asymptotic relation

$$\varepsilon = \alpha_w^2/2 + \alpha_w^3 + \mathcal{O}\left[\alpha_w^4\right] \tag{73}$$

or

$$\beta_w = \frac{\sqrt{2}}{\alpha_w} + \sqrt{2} + \frac{5}{\sqrt{2}}\alpha_w + \frac{3}{\sqrt{2}}\alpha_w^2 + \frac{39}{4\sqrt{2}}\alpha_w^3 + \mathcal{O}\left[\alpha_w^4\right] \tag{74}$$

which confirms and extends the results derived by Peters and Hodges.[12]

V. Summary

The present investigation focused on both the determination of the phenomenological behavior and the derivation of reliable approximations of the natural frequencies, mode shapes, and the buckling limit of very flexible rotating beams. To this end, three different analysis techniques based on power series, singular, and regular perturbation methods, respectively, were introduced and their respective merits were assessed. Note that both the theoretical discussion and the numerical results presented involved the eigenvalues of Eq. (3) which are directly related to both the in-plane and transverse natural frequencies through Eq. (5).

It was first found that although the power series representation, Eq. (7), provides accurate approximations of the eigenvalues, mode shapes, and the buckling limit for most values of the normalized beam stiffness, $\varepsilon = EI/m\Omega^2\bar{R}^4$, it yields no phenomenological insight into the behavior of these dynamic characteristics with respect to the clamping radius a and the parameter ε. Further, it was noted that for very small ε, of the order of 0.001, the determination of the natural frequencies becomes a delicate problem since the exact solution becomes ill conditioned. This difficulty was found to be associated with the change in the structural model as $\varepsilon \to 0$. Specifically, in this limit, the rotating beam becomes a cord for which a different set of boundary conditions applies, i.e., the finiteness of the mode shape at the free edge and a zero displacement at the clamping radius replace the four boundary conditions, Eq. (4).

To clarify the peculiarities of the limiting process $\varepsilon \to 0$, a singular perturbation analysis of the equation of motion Eq. (3) was conducted. Proceeding with this approach, it was assumed that the bending terms were small in comparison to both centripetal and inertia terms over most of the beams length. Then, it was found that boundary layers exist at both ends of the beam. In these small domains, the bending terms are large, comparable to the inertia and centripetal effects. This analysis, which extended and generalized some previously published work, demonstrated that the mode shapes corresponding to a small but nonzero value of ε can be expressed as the sum of their limits as $\varepsilon \to 0$, which represent the mode shapes of a rotating cord, of local perturbations of magnitudes $\varepsilon^{\frac{1}{3}}$, $\varepsilon^{\frac{2}{3}}$, and $\varepsilon^{\frac{5}{6}}$ at the free edge, and $\varepsilon^{\frac{1}{2}}$ at the clamped edge and, finally, of perturbations that affect the entire span of the beam and are proportional to ε, $\varepsilon\,\ell n\,\varepsilon$, ... The closed-form expressions of the corrections of orders up to and including ε and $\varepsilon\,\ell n\,\varepsilon$ are presented to provide a basis for parametric studies.

The eigenvalues of the beam were also investigated. Specifically, it was noted that these values can be expressed as the sum of their limits as $\varepsilon \to 0$ and of perturbations of magnitudes ε^0, $\varepsilon^{\frac{1}{2}}$, and ε^1. The closed-form expressions for the corrections of orders up to and including ε and $\varepsilon\,\ell n\,\varepsilon$ were again derived to easily permit parametric studies.

From a quantitative point of view, it was found that the singular perturbation approximations of both eigenvalues and mode shapes are most reliable when $\varepsilon \ll 1$, as expected, but also for small clamping radii and for low mode numbers. The lack of accuracy of these estimates for high mode numbers has been shown to be rooted in the large magnitude of the corresponding bending term over the entire beam length, not simply in the boundary layers as required by the singular perturbation methodology. In fact, a rough analysis has shown that the relative magnitude of the bending term with respect to the centripetal one increases as n^2 where n is the mode number. The slow degradation of the accuracy of the singular perturbation approximations as the clamping radius a increases can also be attributed to a general increase in magnitude of all derivatives and, in particular, of the bending term. Mathematically, this situation manifests itself by an increase in the relative magnitude of the $\varepsilon^{\frac{1}{2}}$ and ε^1 terms with respect to the ε^0 contribution. Thus, to maintain a constant accuracy it is necessary, as a increases, to increase the order of the perturbation approximation.

The case of a very short beam, $a \approx 1$, was then investigated to provide a better understanding of these shortcomings of the singular perturbation method. In proceeding with this asymptotic analysis it was observed that the entire beam is, for $a \approx 1$, completely within the free edge boundary layer. This observation has led to a transformed version of the original equation of motion, Eq. (3), which admits uniformly valid expansions of the mode shapes and eigenvalues in the form of Eqs. (43) and (44). Surprisingly, this novel regular perturbation scheme was shown by numerical examples to produce extremely reliable estimates for the mode shapes and natural frequencies not only for $a \approx 1$ but for all situations in which the singular perturbation technique was shown to behave poorly, even for $\varepsilon > 1$. For practical applications, the coefficients λ_{-1} and λ_0 of the two-term eigenvalue approximation $\lambda = \lambda_{-1}/\varepsilon^{\frac{1}{3}} + \lambda_0$ have been computed as functions of the unique geometry parameter $\Delta = (1-a)/\varepsilon^{\frac{1}{3}}$ and the results are presented in Figs. 2–4 for the first mode. Given specific values of the clamping radius a and the stiffness ε, the parameter Δ can be computed and the coefficients λ_{-1} and λ_0 can be estimated from either Figs. 2–4 or the asymptotic relations (63), (69), (70), and (72). Then, a reliable approximation of the eigenvalue is obtained from Eq. (55).

Finally, it was noted that the power series, singular, and regular perturbation solutions can also be used to investigate the buckling of rotating beams. Then, it was found that the singular perturbation

method provides accurate approximations of the buckling limit for $a < -1$ but yields no solution for other values of a. On the other hand, the regular perturbation and power series methods were found to be valid for all values of a and to yield estimates of the buckling limit that agree very well with previously published results.

Appendix: Why the Singular Perturbation Method Fails at High Modes

For the singular perturbation method to give accurate results, the leading term in Eq. (3), $\varepsilon X''''(x)$, must be much smaller than the other two, i.e., $-[(1-x^2)X'(x)]'/2$ and $\lambda X(x)$, for all values of x belonging to the outer domain $(a, 1)$. Under this assumption, Eq. (3) reduces to the Legendre differential equation

$$-\frac{1}{2}\frac{\mathrm{d}}{\mathrm{d}x}\left[(1-x^2)\frac{\mathrm{d}X}{\mathrm{d}x}\right] - \lambda X = 0 \tag{A1}$$

the solution of which is $X(x) = P_\nu(x)$ with $\lambda = \nu(\nu+1)/2$.

One way to estimate the importance of each term in Eq. (3) is to compute the two integrals

$$I_1 = \sqrt{\int_a^1 \{\varepsilon P_\nu''''(x)\}^2 \,\mathrm{d}x} \tag{A2}$$

and

$$I_2 = \sqrt{\int_a^1 \left\{\frac{\nu(\nu+1)}{2} P_\nu(x)\right\}^2 \mathrm{d}x} \tag{A3}$$

which approximate the rms values, over the interval $(a, 1)$, of the terms $\varepsilon X''''$ and λX which are, absent and present in the ε^0 outer approximation, respectively. The ratio I_1/I_2 is presented in Table A1 for $a = 0.1$ and $\varepsilon = 0.004$. Note that the value $a = 0.1$ was chosen over the simpler selection $a = 0$ to avoid the presence of the Legendre polynomials $P_n(x)$; the first two of which result in $I_1 = 0$. The results in Table A1 clearly demonstrate that the term $\varepsilon X''''$ has a negligible effect on the outer domain for modes 1 and 2 but contributes to a larger extent for higher modes. Thus, the neglect of the term $\varepsilon X''''$ in the outer domain and, consequently, the use of the singular perturbation technique is only appropriate for the first two modes when $\varepsilon = 0.004$.

A different justification of this phenomenon can be obtained directly from Eq. (3). Specifically, note first that the nth mode possesses $n-1$ zeros in the domain $x \in [a, 1]$. Then, this function could be approximated as

$$X(x) = \cos\left[\frac{(2n-1)\pi(1-x)}{2(1-a)}\right] \tag{A4}$$

Introducing Eq. (A4) into Eq. (A1) it is found that the terms $\varepsilon X''''(x)$ and $[(1-x^2)X'(x)]'/2$ are of order $\varepsilon(n-1)^4$ and $(n-1)^2$, respectively. Thus, the singular perturbation approximation of the nth mode shape will be accurate only if $\varepsilon(n-1)^2 \ll 1$. Equivalently, for any given value $\varepsilon > 0$, there exists a critical mode number over which the singular perturbation technique will fail to provide accurate approximations of the eigenvalues and mode shapes.

Table A1 I_1/I_2 ratio for $a = 0.1$ and $\varepsilon = 0.004$

Mode	I_1/I_2
1	0.0014
2	0.0134
3	0.7554
4	4.7749

Acknowledgment

The authors would like to thank the AlliedSignal Aerospace Corporation for their support to the first author under its Doctoral Fellowship Program.

References

[1]Leissa, A., "Vibrational Aspects of Rotating Turbomachinery Blades," *Applied Mechanics Reviews*, Vol. 34, No. 5, 1981, pp. 629–635.

[2]Bramwell, A. R. S., *Helicopter Dynamics*, Vol. 3, Wiley, New York, 1976, p. 307.

[3]Colin, A. D., "Modal Analysis for Liapunov Stability of Rotating Elastic Bodies," Ph.D. Dissertation, Univ. of California, Los Angeles, CA, 1973, pp. 11–43.

[4]Peters, D. A., "An Approximate Solution for the Free Vibrations of Rotating Uniform Cantilever Beams," NASA TM X-62,299, Sept. 1973.

[5]Lakin, W. D., "On the Differential Equation of a Rapidly Rotating Slender Rod," *Quarterly of Applied Mathematics*, Vol. 32, No. 1, 1974, pp. 11–27.

[6]Lakin, W. D., and Ng, B. S., "A Fourth-Order Eigenvalue Problem With a Turning Point at the Boundary," *Quarterly Journal of Mechanics and Applied Mathematics*, Vol. 28, Pt. 1, Feb. 1975, pp. 107–121.

[7]Hodges, D. H., "An Approximate Formula for the Fundamental Frequency of a Uniform Rotating Beam Clamped off the Axis of Rotation," *Journal of Sound and Vibration*, Vol. 77, No. 1, 1981, pp. 11–18.

[8]Nachman, A., "The Buckling of Rotating Rods," *Journal of Applied Mechanics*, Vol. 42, Ser. E, No. 1, 1975, pp. 222–224.

[9]Lakin, W. D., "Vibrations of a Rotating Flexible Rod Clamped off the Axis of Rotation," *Journal of Engineering Mathematics*, Vol. 10, No. 4, 1976, pp. 313–321.

[10]Lakin, W. D., and Nachman, A., "Unstable Vibrations and Buckling of Rotating Flexible Rods," *Quarterly of Applied Mathematics*, Vol. 35, No. 4, 1978, pp. 479–493.

[11]Lakin, W. D., and Nachman, A., "Vibration and Buckling of Rotating Flexible Rods at Transitional Parameter Values," *Journal of Engineering Mathematics*, Vol. 13, No. 1, 1979, pp. 339–346.

[12]Peters, D. A., and Hodges, D. H., "In-Plane Vibration and Buckling of a Rotating Beam Clamped Off the Axis of Rotation," *Journal of Applied Mechanics*, Vol. 47, No. 2, 1980, pp. 398–402.

[13]Lakin, W. D., Mathon, R., and Nachman, A., "Buckling and Vibration of a Rotating Spoke," *Journal of Engineering Mathematics*, Vol. 12, 1978, pp. 193–206.

[14]Lakin, W. D., and Nachman, A., "Uniform Real-Variable Asymptotic Approximations for Vibrations of a Rotating Flexible Rod," *SIAM Journal of Applied Mathematics*, Vol. 42, No. 1, 1982, pp. 77–85.

[15]Stafford, R. O., and Giurgiutiu, V., "Semi Analytic Methods for Rotating Timoshenko Beams," *International Journal of Mechanical Sciences*, Vol. 17, 1975, pp. 719–727.

[16]Giurgiutiu, V., and Stafford, R. O., "Semi Analytic Methods for Frequencies and Mode Shapes of Rotor Blades," *Vertica*, Vol. 1, No. 4, 1977, pp. 291–306.

[17]Wright, A. D., Smith, C. E., Thresher, R. W., and Wang, J. L. C., "Vibration Modes of Centrifugally Stiffened Beams," *Journal of Applied Mechanics*, Vol. 49, No. 1, 1982, pp. 197–202.

[18]Nayfeh, A., *Introduction to Perturbation Techniques*, 1st ed., Wiley, New York, 1981, pp. 257–324.

[19]Mignolet, M. P., and Harish, M. V., "Particular Solutions of a Class of Nonhomogenous Laplace Ordinary Differential Equations Encountered in Perturbation Analyses," *Zeitschrift fur angewandte Mathematik und Mechanik*, Vol. 75, No. 4, 1995.

[20]Abramowitz, M., and Stegun, I. A., *Handbook of Mathematical Functions*, 9th ed., Dover, New York, 1972, Chaps. 8–10.

[21]Lebedev, N. N., *Special Functions and Their Applications*, 1st ed., Dover, New York, 1972, p. 167.

[22]Rothman, M., "Tables of the Integrals and Differential Coefficients of Gi(+x) and Hi(−x)," *Quarterly Journal of Mechanics and Applied Mathematics*, Vol. 7, Pt. 3, 1954, pp. 378–384.

[23]Wolfram, S., *Mathematica : A System for Doing Mathematics by Computer*, 2nd ed., Addison–Wesley, New York, 1991, p. 575.

[24]White, W. F., Kvaternik, R. G., and Kaza, K. R. V., "Buckling of Rotating Beams," *International Journal of Mechanical Sciences*, Vol. 21, No. 12, 1979, pp. 739–745.

[25]Eick, C. D., "Free Vibration of Flexible Rotating Beams and Plates," Ph.D. Dissertation, Arizona State Univ., Tempe, AZ, 1994.